



Performance analysis of portable HEPA filters and temporary plastic anterooms on the spread of surrogate coronavirus

Ehsan S. Mousavi^{a,*}, Krystal J. Godri Pollitt^b, Jodi Sherman^c, Richard A. Martinello^d

^a Department of Construction Science and Management, Clemson University, 2-132 Lee Hall, Clemson, SC, 29634, USA

^b Environmental Health Sciences, Yale School of Public Health, New Haven, CT, 06520, USA

^c Associate Professor of Anesthesiology, Yale School of Medicine, and Associate Professor of Epidemiology in Environmental Health Sciences, Director, Program in Healthcare Environmental Sustainability, Yale School of Public Health, New Haven, CT, 06520, USA

^d Department of Internal Medicine and Pediatrics, Yale School of Medicine. Department of Infection Prevention, Yale New Haven Health, New Haven, CT 06510, USA

ARTICLE INFO

Keywords:

ARS-CoV-2
Hospital
Isolation room
HEPA filter
Coronavirus
COVID-19
Air quality
Negative pressure room

ABSTRACT

The outbreak of COVID-19, and its current resurgence in the United States has resulted in a shortage of isolation rooms within many U.S. hospitals admitting COVID-19-positive cases. As a result, hospital systems, especially those at an epicenter of this outbreak, have initiated task forces to identify and implement various approaches to increase their isolation capacities. This paper describes an innovative temporary anteroom in addition to a portable air purifier unit to turn a general patient room into an isolation space. Using an aerosolization system with a surrogate oil-based substance, we evaluated the effectiveness of the temporary plastic anteroom and the portable air purifier unit. Moreover, the optimal location of the portable unit, as well as the effect of negative pressurization and door opening on the containment of surrogate aerosols were assessed. Results suggested that the temporary anteroom alone could prevent the migration of nearly 98% of the surrogate aerosols into the adjacent corridor. Also, it was shown that the best location of a single portable air purifier unit is inside the isolation room and near the patient's bed. The outcome of this paper can be widely used by hospital facilities managers when attempting to retrofit a general patient room into an airborne infection isolation room.

1. Introduction

Worldwide, SARS-CoV-2 has caused over 18 million infections and has led to nearly 700,000 deaths as of August 05, 2020 [1]. Similar to other highly pathogenic coronaviruses, SARS-CoV-2 has been associated with outbreaks of healthcare associated infections in nursing homes [2] and hospitals [3]. While the mode of transmission of SARS-CoV-2 from person to person remains unknown, it is expected that the primary route of transmission is by respiratory droplets and possibly small aerosols [4, 5]. The Centers for Disease Control and Prevention (CDC) recommends that hospitalized persons be placed in a single person room with the door kept closed, and that an airborne infection isolation room (AIIR), also known as a negative pressure room, be used for such patients who may require an aerosol generating procedure in an effort to contain potentially infectious aerosols from patients known or suspected of an active infection due to SARS-CoV-2 [6]. However, as was seen in Italy [7], the US [8] and in other countries [9], the first wave of the SARS-CoV-2 pandemic often quickly saturated the capacity of hospitals to provide

an AIIR for all patients known to have or suspected of COVID-19.

Beyond acute care hospitals, nursing facilities typically have little to no capacity to provide an AIIR for patients. Instead, nursing facilities tend to transfer patients suspected of an infectious disease transmitted by small particle aerosols to a hospital for care and isolation in an AIIR for the duration of the period the patient may be contagious. During the first wave of the SARS-CoV-2 pandemic, with both nursing facilities and hospitals often overwhelmed in regions that experienced the greatest prevalence of COVID, these hospital resources were not available. Patients suspected or known to have COVID were unable to be isolated in the nursing facility. Or, if transferred to a hospital, they were cared for in a room with neutral pressure rather than an AIIR. Neutral pressure rooms are not designed to contain potentially infectious aerosols and the placement of a patient with COVID in a neutral pressure room may place non-infected patients and staff at risk of exposure, both because of these aerosols migrating outside of the room and since the conditioned air in patient rooms is recirculated rather than exhausted outside as is the case for air in an AIIR. This risk is further compounded by most commercial

* Corresponding author.

E-mail address: mousavi@clemson.edu (E.S. Mousavi).

<https://doi.org/10.1016/j.buildenv.2020.107186>

Received 23 July 2020; Received in revised form 6 August 2020; Accepted 7 August 2020

Available online 13 August 2020

0360-1323/© 2020 Elsevier Ltd. All rights reserved.

buildings, including hospitals, recirculating 80% or more of the air in a forced air system [10]. While US hospital construction standards require a minimum of MERV 13 or MERV 14 filtration for both fresh and recirculated air [11], this level of filtration is not capable of reliably removing viral particles.

A recent assessment of acute care hospitals in the US showed that less than 6% of the 788,032 hospital beds were in isolation rooms; approximately 1.4 isolation beds per 10,000 persons [12]. The availability of acute care hospital beds in the US designed for the isolation of patients with airborne transmissible infectious diseases has changed little since the US Government Accounting Office's assessment for the country's preparedness for a response to bioterrorism in 2003 [13].

With this lack of capacity of AIIR, the CDC has suggested the use of portable fan systems with HEPA filtration to provide surge capacity during a pandemic or other crises [6,14]. Depending on the installation, these units can (i) clean the indoor air by filtering pathogens from the space, and (ii) create negative pressure in the space to prevent pathogens from spreading into adjacent space. These effects have shown to be somewhat independent [15,16]. However, the overall performance of such portable HEPA units, change in efficiency over time, and optimal placement has not been sufficiently investigated, and still remains challenging [17]. Moreover, anterooms were shown to be effective in

containing airborne infectious particles by adding another layer of physical barrier to the AIIR [18,19]. CDC also supports the use of an anteroom with a positive pressure with respect to the AIIR, and negative pressure with respect to the adjoining corridor for patients with highly contagious respiratory problems (i.e., TB and SARS) [20]. We performed an experimental study to determine the effectiveness and ideal placement of portable HEPA units. We also evaluated the effectiveness of negative pressurization, as well as a temporary anteroom structure on minimizing the dispersion of contaminants in the hospital space.

2. Method

2.1. Experimental setup

A series of experiments were conducted in a healthcare facility located in the Southeast region of the US to study the spread of surrogate aerosols for a patient room equipped with a temporary anteroom with plastic barrier (Fig. 1). The patient room was decommissioned at the time for cosmetic renovation and repair. The room was 6.3 m (L) x 3.9 m (W) x 3.0 m (H) and connected to the hallway that had a wood door that was sealed from other adjacent spaces with block walls and drywall ceilings. A temporary plastic barrier was installed inside the room, 4.0 m

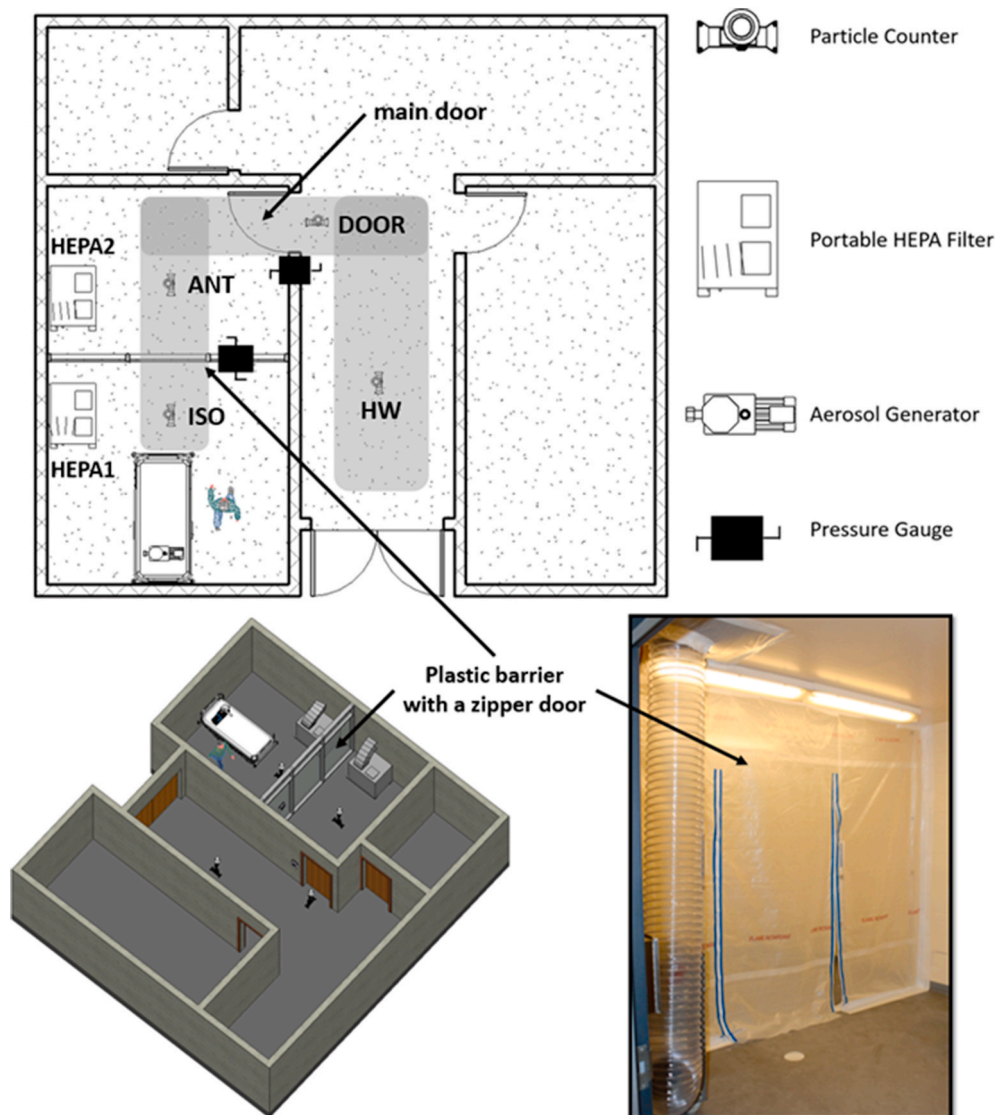


Fig. 1. Experimental setup, sampling location, and the plastic barrier.

away from the entrance to the patient room and divided the room into an isolation room (ISO) and an anteroom (ANT). The link shows an animation of the experimental setup (<https://youtu.be/R9EQEfJFoel>). Two portable High Efficiency Particulate Air (HEPA) machines (Abatement Technologies®PAS2400) equipped with brand-new HEPA filters, were used to establish various pressurization schemes across the plastic barrier and the main door (Fig. 1). When turned on, the HEPA machines drew air at a $1500 \text{ m}^3 \text{ h}^{-1}$ rate and discharged the filtered air to the outdoors. One HEPA machine produced 20 air changes per hour (ACH) in the entire room (i.e., ISO + ANT). One could also calculate individual ACHs for ISO and ANT by dividing the flow rate of the HEPA machine by the volume of each space, which would result in 30 and 55 ACH for ISO and ANT, respectively. These numbers are not additive, meaning that the combined ACH is not equal to the sum of individual ACH. Therefore, our calculations in Table 1 were based on a rate of 20 ACH per HEPA machine. It must be also noted that while there are no guidelines for portable HEPA machine ACH selection, the specific machine used in this work was on the higher end of commercially available flow rates and produced ACHs that were higher than the hospital design setpoint for airborne infection isolation rooms [21] (i.e., 12 ACH).

Two OmniGuard 5 DPM pressure monitoring devices, one at the plastic barrier and one at the main door, were used to monitor the space pressurization throughout the tests. An oil-based substance (BIS-2-ethylhexyl sebacate) was used to generate aerosols using a pharmaceutical nebulizer (Rescoe Medical Portable Travel Nebulizer System, model – NEB-PORT) connected to an air pump with a constant power throughout the experiments. Aerosols were released into the space at the patient bed where the patient's head is located, to simulate the spread of SARS-CoV-2 virus from an infected patient. While the exact rate of aerosol generation was not calculated, the same aerosolization procedure was maintained for all the tests, and resulted in concentrations that were nearly 1000 times of those of the background measurements (<1000 of $0.3 \mu\text{m}$ particles per liter). This rate was intentionally much higher ($0.3 \mu\text{m}$ aerosol diameter in the order of 10^5 particles/liter) than the rate of virus spread due to respiratory activities (~ 6000 particles/per cough) [22] to create sufficient contrast in the data. During the first round of experiments, four different pressure cases were tested based on the on/off permutation of the HEPA machines. No experiment was performed in the absence of the plastic barrier since it was already installed prior to the tests.

As can be seen in Table 1, the HEPA machines were able to produce negative pressures greater or equal to that recommended by the CDC and ASHRAE standards (-2.5 Pa). Table 1 shows the airflow conditions for these tests (i.e., Tests 1–4), while other parameters (e.g., geometry of tests) were held constant. When the first round of experiments was complete, the research team added three more testing scenarios by (a) intentionally leaving the zipper door half open (Test 5), (b) leaving an open space underneath the zipper door (Test 6), and (c) making a 15 cm tear in the plastic barrier (Test 7). These scenarios were designed to test the integrity of the temporary system in the presence of potential damage (Table 1 and Fig. 2). For brevity tests were also named after the configuration of HEPA units in the isolation room and anteroom respectively. For example, the HEPA 1 was on, and HEPA 2 was off case is also called the ON-OFF case (i.e., Test 2).

Table 1
HEPA machine Configurations and pressure relationships (ΔP).

TEST #	Abbreviations	Configuration	HEPA 1	ΔP ISO→ANT	HEPA 2	ΔP ANT→HW	Total ACH
Test 1	ON-ON	ISO-HEPA-ON Cases	ON	-12.0 Pa	ON	-5.0 Pa	40 ACH
Test 2	ON-OFF		ON	-4.0 Pa	OFF	-2.5 Pa	20 ACH
Test 3	OFF-ON	ISO-HEPA OFF Cases	OFF	0.0 Pa	ON	-2.5 Pa	20 ACH
Test 4	OFF-OFF		OFF	0.0 Pa	OFF	0.0 Pa	0 ACH
Test 5	Damage Cases		ON	-1.5 Pa	ON	-3.0 Pa	40 ACH
Test 6			ON	-1.5 Pa	ON	-5.0 Pa	40 ACH
Test 7			ON	-4.5 Pa	ON	-5.0 Pa	40 ACH

2.2. Test procedure

Experiments were designed to simulate a typical visit with an infected patient. Background concentrations of particles were measured for 2 min prior to aerosolization. Next, a person waited at the patient's bed for 90 s to simulate a typical visit to check the vital signs of a patient. Then the person walked out of the room toward the hallway and waited for another 45 s at 4.0 m away from the main door (HW). Finally, the person walked backed into the room, and this procedure recurred three times to assure the repeatability of experiments and consistency in data measurements (Table 2). The grey shade in Fig. 1 shows the walking pathway. The entire process was timed by the person, as well as an independent observer. The observer also timed the duration of door opening cycle at each incident. On average it took 5.85 s ($\sigma = 0.3$), and 4.5 s ($\sigma = 0.2$) for the plastic zipper and main door openings, respectively.

Concentration of particles were measured using ExTech VPC300 hand-held particle counters with a 2.83 L/min flowrate and a coincidence loss of 5% at 7×10^4 particles per liter, per the manufacturer manual. The particle counters (PC) were placed in the walking pathway inside the isolation room (PC-ISO), in the temporary anteroom (PC-ANT), at the main door (PC-DOOR), and in the hallway (PC-HW). It must be noted that the term 'PC' is dropped from the name of the particle counters throughout the paper. For example, DOOR refers to the PC-DOOR sampling location and does not indicate a specific door. For tests 5 and 6, PC-HW was placed directly in front of the plastic damage (i.e., 15 cm tear, open zipper). Therefore, concentrations outside the room were only measured at the DOOR station. Air parcels were sampled approximately every 15 s for the duration of the experiments. In fact, extra data points were collected after the experiment completed ($t > 12:30$) to capture any random pattern that might have occurred post-procedure. The particle counters were capable of measuring aerosols with the diameter range of $0.3\text{--}10.0 \mu\text{m}$ in six different channels. For this study, only the concentration of the $0.3 \mu\text{m}$, $1.0 \mu\text{m}$, and $3.0 \mu\text{m}$ particle size channels were measured, with an emphasis on the $0.3 \mu\text{m}$ size, as this size is the closest to the size range of SARS-CoV-2 virus (i.e., $0.2\text{--}0.3 \mu\text{m}$). Respectively, these three bins represent fine, intermediate, and large particle size, and cover a range from the virus nuclei to virus carrying on a light droplet.

2.3. Statistical analysis

The test procedure for each case was repeated three times to ensure the consistency of the test results. ANOVA tests were conducted for the data collected at each sampling point, and for each test to evaluate the consistency in the data. The null hypothesis was that the aerosol distributions for each repetition were similar and it was rejected for a p-value less than 0.05, corresponding to a 95% confidence interval. Except for two cases (Test2 [ON-OFF]-ISO, and Test2 [ON-OFF]-DOOR), the outcome ($p\text{-value} > 0.05$) showed that the data were consistent with 95% confidence interval. While the results were reasonably consistent for all the cases, the p-values were generally higher for the cases when the HEPA machine was off (i.e., Tests 3 and 4), showing that the removal mechanism could introduce randomness to the dataset (Table 3).

In order to study the dispersion of the aerosols, one should subtract

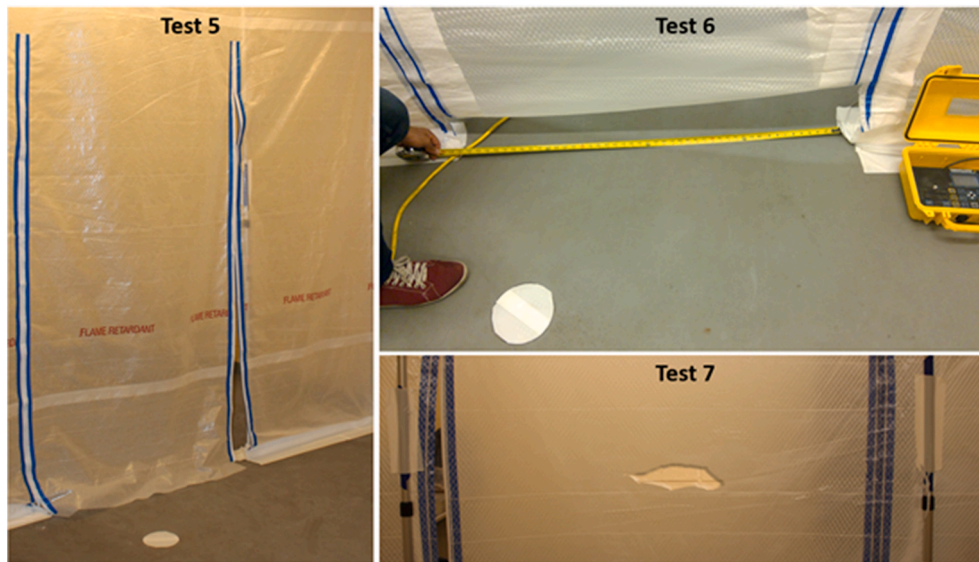


Fig. 2. Intentional Damage to Plastic Barrier by leaving the zipper door half-open (Test 5), leaving a space underneath the zipper door (Test 6), and tearing the Plastic Barrier (Test 7).

Table 2
Test procedure.

Row	Activity	Start Time [min:sec]	Finish Time [min:sec]	Door opening
1	Background Measurements	0:00	2:00	
2	Aerosolization	2:00	2:30	
3	Wait in the Room	2:30	4:00	
4	Walk Toward Hallway	4:00	4:15	Plastic and main door open
5	Wait in the Hallway	4:15	5:00	
6	Walking Toward Room and wait	5:00	5:30	Plastic and main door open
7	Repeat activities #2-6	5:30	9:00	
8	Repeat activities #2-6	9:00	12:30	

the effect of background concentrations. To that end, the background concentrations were subtracted from the measurements prior to further analysis. Also, the exposure to background was defined as the area under the concentration-time curve during the background data collection (Eq. (1)). In general, one could define exposure from any reference point t_0 in a similar fashion (Eq. (2)).

$$E_{BG} = \int_{t=0}^{2:00} C(t)dt \tag{1}$$

$$E(t) = \int_{t_0}^t C(t)dt \tag{2}$$

where E is exposure, E_{BG} is background exposure, and C(t) is the concentration as a function of time. It must be further noted that the notion of exposure has been defined in the same manner in the literature [23,

Table 3
Results of the Analysis of Variance Test (p-values) four Test Settings in All Sampling Locations; 95% Confidence Interval.

Particle Counter Sampling Station	Test 1 (ON-ON)	Test2 (ON-OFF)	Test 3 (OFF-ON)	Test 4 (OFF-OFF)
ISO	0.05	0.02	0.53	0.81
ANT	0.07	0.09	0.88	0.92
DOOR	0.08	$<10^{-3}$	0.68	0.71
HW	0.25	0.14	0.58	0.27

24]. Another parameter was defined to quantify the time it took for the sensors to detect the generated aerosols. Therefore, the lag (δ) was defined as the time difference between the end of aerosolization and the first significant measurement (peak) over background. Further, the migration ratio (ϵ) characterizing the migration of particles from one space (A) to another (B) is given by Eq. (3).

$$\epsilon_{A \rightarrow B} = \frac{\int_{t=2:00}^{12:30} C(t)_A dt}{\int_{t=2:00}^{12:30} C(t)_B dt} \tag{3}$$

The migration rate can be defined for any two spaces and they don't necessarily have to be neighbors. By definition, the migration rate from a space to itself ($\epsilon_{ISO \rightarrow ISO}$) is one, and it is used as a basis of comparison.

3. Results and discussion

3.1. Spatial distribution of aerosols

Concentration of particles rapidly increased at the onset of aerosolization inside the isolation space (Fig. 3). For the cases where the HEPA machine inside the isolation space was on, the ISO concentration was reduced until the next aerosolization indicating effectiveness of HEPA filtration. Conversely, particle concentrations seemed to reach the saturation point where the volumetric concentration could no longer increase in the air, and hence, ISO concentrations behaved almost asymptotically. This phenomenon was more noticeable for the ISO-HEPA-OFF cases. Though not conspicuous on the logarithmic scale (Fig. 3), particle concentrations decreased up to 50% of the steady concentration when the ISO-HEPA was turned on, showing that the HEPA machine effectively removed particles from the isolation space.

Other stations also sensed some concentrations, however the spread of aerosols was significantly different for each test setting. Regardless, three distinct patterns were observed for all cases: (a) there was a remarkable drop in the average concentration of particles in all the stations outside the isolation space; (b) the distribution patterns followed similar patterns outside the room (i.e., at PC-DOOR and PC-HW), indicating that there was no control over the particles that were able to escape the room; and (c) significant accumulation of particles was observed when the HEPA machines were both off (i.e., Test 4), suggesting the important role of filtration in maintaining the air cleanliness.

These patterns were observed for all three aerosol size bins, though the migration rate was increased for smaller aerosol size (Fig. 4).

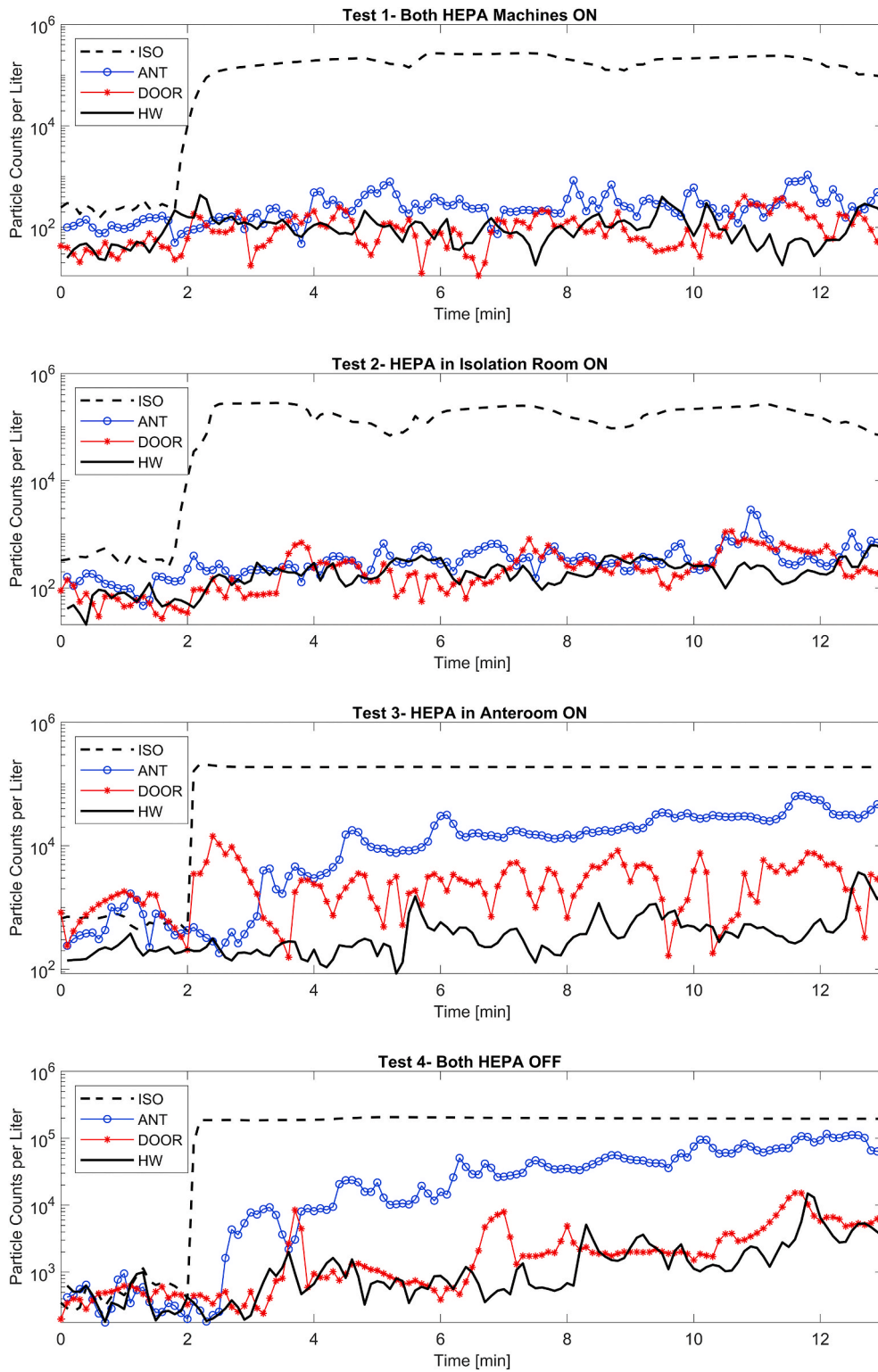


Fig. 3. Particle Counts per liter Curves for all locations and tests. The Y-axis uses the Logarithmic Scale.

Specifically, for all test configurations, the highest migration rate was associated with the $0.3 \mu\text{m}$ size. The migration rate decreased an order of magnitude for the $3.0 \mu\text{m}$ size aerosols, indicating the high mobility of fine aerosols. Further, the migration rate from the isolation space to the anteroom ($\epsilon_{\text{ISO} \rightarrow \text{ANT}}$), seemed to be more profound for $0.3 \mu\text{m}$ aerosols. Migration ratio lines tend to have very similar slopes from ANT to DOOR to HW sampling stations. This was not particularly the case for Test 3 where the HEPA unit was placed in the anteroom. In that case, the

anteroom was effectively cleaned by the HEPA unit, again leading to lower migrations rates for larger particle sizes (Fig. 4).

3.2. Effect of plastic barrier

In general, the experimental design offered three states between the neighboring sampling stations: (a) plastic barrier between ISO and ANT; (b) solid door between ANT and DOOR; and (c) no barrier between

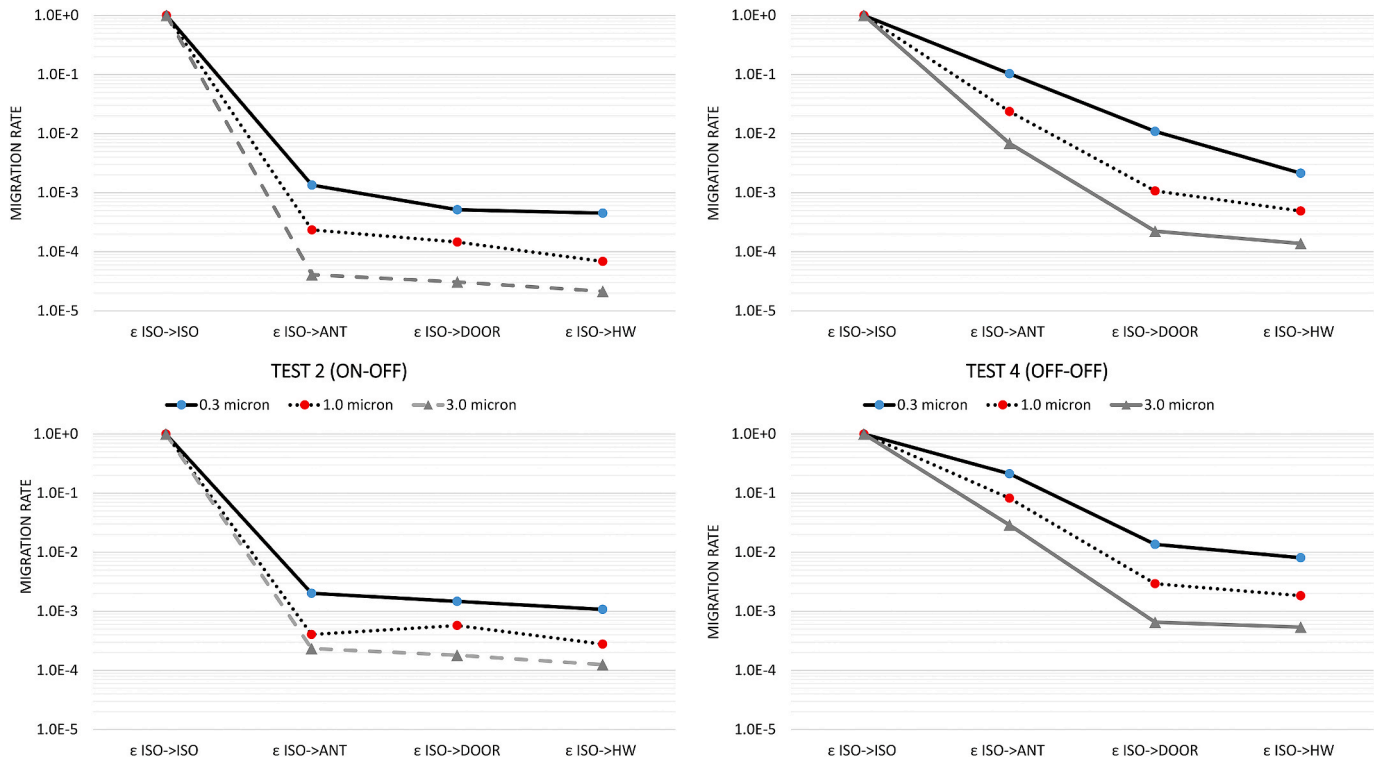


Fig. 4. Migration Rates from the isolation spaces for different particle sizes.

DOOR and HW. Results show that the concentration of particles measured at the DOOR and HW stations were similar, showing that particles readily dispersed when there was no physical barrier. Conversely, the plastic barrier was an effective barrier in containing the particles inside the isolation space. Results showed that even under no pressurization/filtration scheme, only 20% of particles in the isolation space were detected in the anteroom (Fig. 5). The containment achieved by the plastic barrier was even better than that for the solid door. Specifically, door opening created drastic changes in the airflow patterns that led to the migration of particles into the hallway even in the presence of negative pressure. This finding is consistent with the literature on large air mixing due to swing door openings [25–27]; the results here for the plastic zipper closure are rather similar to a sliding door which has been shown to be less disruptive [28,29]. Upon aerosolization, a plume of aerosols was immediately detected in the isolation space. However, the plastic barrier caused a lag in the time particles were sensed in the anteroom. This lag was also a function of negative pressurization at the plastic barrier, but even under no pressurization (Test 4, OFF-OFF) there was a 1-min lag in particle migration into the anteroom. This lag was 2 min at DOOR and HW, again indicating that no

barrier led to no lag.

3.3. Effect of pressurization

Negative pressure impacted the efficiency of the plastic barrier. For the ISO-HEPA-ON cases (i.e., tests 1 and 2), the migration ratio was less than 1%. Interestingly, increasing ΔP from 4.0 Pa (i.e., Test 2) to 12Pa (i.e., Test 1) did not have a significant impact on the migration rate, suggesting that over-pressurization did not provide extra containment. On the contrary, while conducting these experiments, it was observed that high negative pressures can easily jeopardize the structural integrity of the plastic barrier. In fact, prior to Test 1, the research team intended to also test the 25 Pa negative pressure. But such ΔP 's were so powerful and almost collapsed the plastic barrier mounted on ceiling tight aluminum shores. Tests 3 and 4 had no pressure differential across the plastic barrier, yet the HEPA machine in the anteroom was effective in removing the particles from the anteroom through HEPA filtration, reducing the average concentration in ANT to half that in ISO (Table 4). Unlike the plastic door, the negative pressure across the solid door was not similarly effective. For instance, for the ON-ON case (Test 1) and despite 5.0 Pa negative pressure, 38% of particles in the anteroom dispersed to the hallway. This value was less than 1% across the plastic barrier.

The negative pressure magnitude alone was not the only important parameter; how it was achieved was equally important. For example, the negative pressure at the solid door in Test 2 (ON-OFF) was not produced directly in the anteroom (HEPA 2 was off). Rather, it was a byproduct of the HEPA machine in the isolation space. Thus, it did not provide any real protection at the solid door as indicated by a migration ratio of 62.6%. Further, solid door swings induced large wakes in the airflow that facilitated further migration into the hallway. This phenomenon could profoundly impact the containment of particles in the anteroom. In fact, the spikes in particle counts due to door operation were associated with dispersion into the hallway (Fig. 6). These spikes took place with a few minutes lag in some occasions (e.g., ANT in Test 2) which could be due to potential transient effects such as human walking.



Fig. 5. Migration rates for all tests and all neighboring sampling locations.

Table 4
Average particle concentrations over background and migration rate (ϵ) for sampling locations.

	C_{ISO}	C_{ANT}	$\Delta P_{ISO \rightarrow ANT}$	$\epsilon_{ISO \rightarrow ANT}$	C_{DOOR}	$\Delta P_{ANT \rightarrow DOOR}$	$\epsilon_{ANT \rightarrow DOOR}$	C_{HW}	$\epsilon_{DOOR \rightarrow HW}$
TEST 1 (ON-ON)	190,345	301	-12.0 Pa	0.13%	98	-5.0 Pa	32.56%	86	87.52%
TEST 2 (ON-OFF)	180,057	409	-4.0 Pa	0.20%	265	-2.0 Pa	62.59%	194	73.15%
TEST 3 (OFF-ON)	184,203	18,943	0.0 Pa	10.28%	2006	-2.0 Pa	10.59%	394	19.65%
TEST 4 (OFF-OFF)	190,635	40,580	0.0 Pa	21.29%	2591	0.0 Pa	6.39%	1537	59.33%

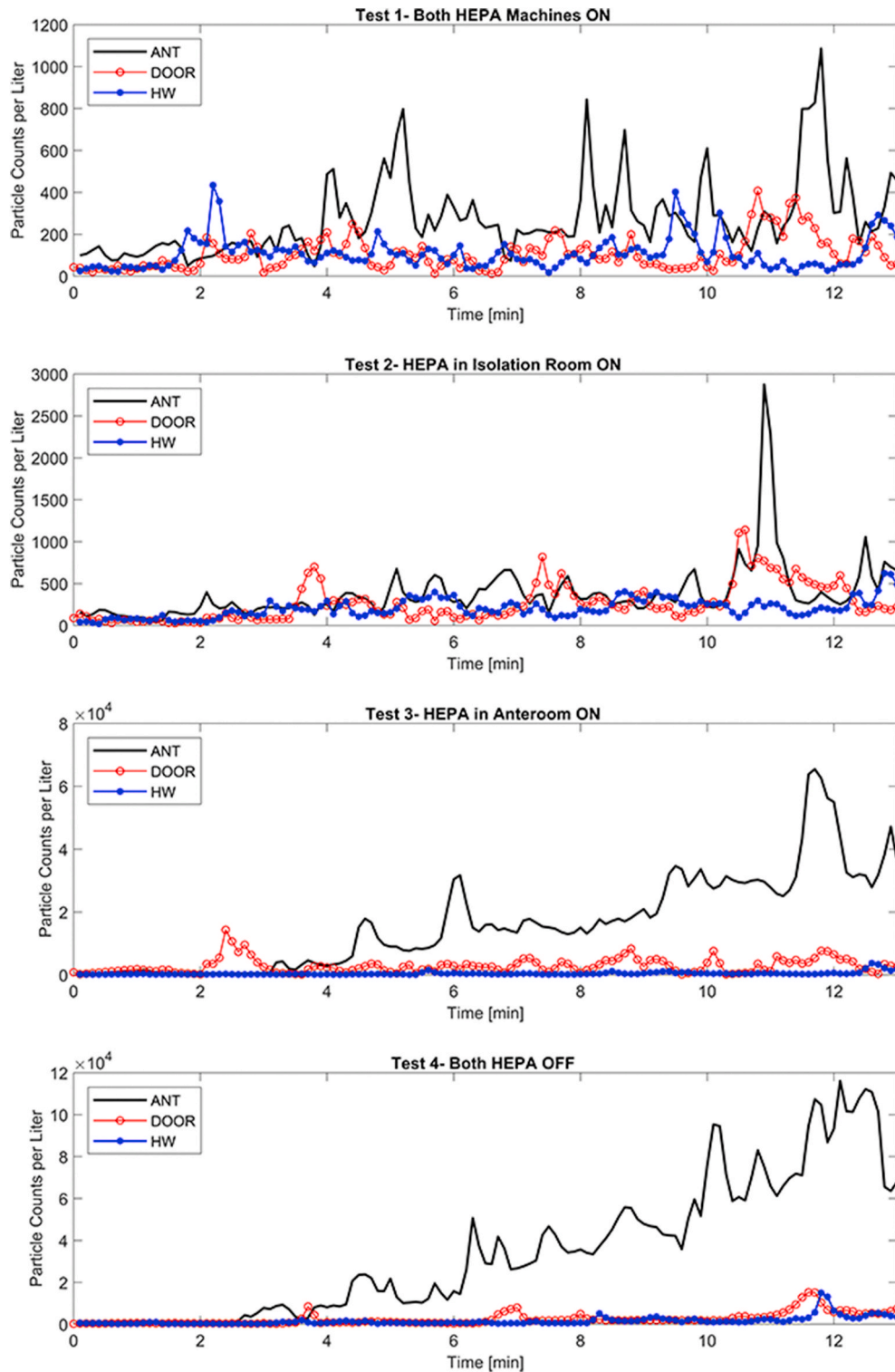


Fig. 6. Counts of Particles per liter outside the Isolation Space vs. Door Operation.

Further, the movement of the swing door as a large solid body could create significant wakes inside the anteroom and the corridor, which in turn, could result in a lagged spike in the concentration curve. This phenomena could be more significant when the air movement due to door opening is stronger than the general flow of air in a non-mixed or under-ventilation room.

3.4. Effect of anteroom

The effect of anteroom on the overall migration of particles is interesting from two perspectives: 1) the sole effect of anteroom as another protective layer, and 2) the effect of air cleanliness (HEPA machine) on the performance of the anteroom. As stated in the methods section, we did not conduct experiments with no plastic barrier, so it was not possible to compare anteroom vs. no-anteroom cases. However, the migration patterns from the anteroom to outside the room could be similar to a hypothetical case where the isolation space was the anteroom and it was directly connected to the hallway (we labeled this as “absence of anteroom” in Table 5) Therefore, one could compare $\epsilon_{ANT->DOOR}$ to $\epsilon_{ISO->DOOR}$ as a surrogate to study the performance of anteroom. Results shown in Table 6 demonstrate that adding another layer of protection was profoundly effective in containing contamination. Even under no HEPA filtration (i.e., Test 4), the plastic barrier could reduce the migration ratio nearly four times.

Fig. 7 shows particle counts per liter in the anteroom. The results are very similar for the ISO-HEPA-OFF, and ISO-HEPA-ON cases. A comparison between Test 2 (ON-OFF) and Test 3 (OFF-ON) is particularly interesting since in both cases only one portable HEPA machine was on, but at a different location. The results of the OFF-ON case demonstrated that placing the HEPA machine in the anteroom drew the particles from ISO to ANT. This pathway is not desirable as it increased the probability of particle leakage into the hallway. In particular, the concentration of particles at ANT for Test 3 and Test 2 was increased 50-times. This count at DOOR in the OFF-ON case was nearly ten times that of the ON-OFF case. This happened despite negative pressure at the solid door suggesting that while negative pressure is important, it must be considered within the overall design context.

3.5. Effect of defects in the plastic barrier

Three specific tests were designed to assess the effect of potential damage to the plastic barrier on the spread of particles. Both HEPA machines were operating during these tests. Nonetheless, the openings on the plastic barrier (e.g., half-open zipper, or a hole) drastically changed the pressure differential across the plastic barrier. Our measurements show that even a 15 cm tear on the surface of the plastic wall almost halved the pressure difference (Table 1). Compared to Test 1, the damage to the plastic barrier triggered higher rates of migration into the anteroom (Fig. 8). However, Test 6 (i.e., small open space under the zip door) seemed to have lower impact as the opening was close to the floor level. This can be attributed to the fact that small particles tend to follow air streamlines. One explanation for these observations is that smaller particles tend to remain suspended in higher elevations. The other two cases of damage (Tests 5 and 6) had higher rates of migration. Again, high spikes were mostly associated with door openings (Fig. 8). The

Table 5

The effect of anteroom on aerosol containment under various filtration strategies.

	Presence of Anteroom		Absence of Anteroom	
	$\Delta P_{ISO->ANT}$	$\epsilon_{ISO->DOOR}$	$\Delta P_{ANT->DOOR}$	$\epsilon_{ANT->DOOR}$
TEST 1 (ON-ON)	-12.0 Pa	0.05%	-5.0 Pa	32.56%
TEST 2 (ON-OFF)	-4.0 Pa	0.12%	-2.0 Pa	62.59%
TEST 3 (OFF-ON)	0.0 Pa	1.08%	-2.0 Pa	10.59%
TEST 4 (OFF-OFF)	0.0 Pa	1.36%	0.0 Pa	6.39%

Table 6

Average particle concentrations over background and migration rate (ϵ) for the damage cases.

	C_{ISO}	C_{ANT}	$\Delta P_{ISO->ANT}$	$\epsilon_{ISO->ANT}$	C_{DOOR}	$\Delta P_{ANT->DOOR}$	$\epsilon_{ISO->ANT}$
TEST 1	190,345	301	-12.0 Pa	0.13%	98	-5.0 Pa	39.84%
TEST 5	188,116	600	-1.5 Pa	0.32%	416	-3.0 Pa	69.36%
TEST 6	186,783	243	-1.5 Pa	0.13%	158	-5.0 Pa	65.11%
TEST 7	217,009	616	-4.5 Pa	0.28%	434	-5.0 Pa	70.40%

average concentrations of particles for the damage cases were higher than that for Test 2, suggesting that the combination of a faulty barrier and a HEPA machine in the anteroom could draw particles outside of the isolation space. Regardless, these concentrations were orders of magnitude lower than what was observed in Test 4 (i.e., OFF-OFF case).

As can be seen in Table 6, while the performance of the damage cases was not as good as the Test 1, the damaged plastic barriers still provided reasonable containment. In fact, the migration rate ($\epsilon_{ISO->ANT}$) was less than half a percent for all the damage cases. Although perfect sealing must be practiced for these temporary plastic barriers, small spaces underneath the zipper door did not lead to any additional migration. Open zipper and holes in the plastic barrier on the other hand must be avoided to the extent possible.

4. Conclusions

In the event of an outbreak, such as the current SARS-CoV-2 virus, the hospital ventilation system typically supports isolation spaces where contagious patients are admitted. These rooms are designed to contain and remove pathogenic agents quickly. In the surge of patients though, there may be insufficient numbers of rooms of this kind, as several countries such as Italy, the US, and China have experienced [30–33]. Therefore, innovative measures must take place to better prepare the hospital system for an airborne pandemic. In response, this study explored the performance of a temporary anteroom with and without portable HEPA filtration machines on the containment and removal of surrogate particles. These plastic barriers are cheap, easy and quick to install. Hospitals, especially those located in an epicenter of the outbreak, are currently very busy treating COVID patients as they arrive on a daily basis. This fact has put these hospitals in a fragile position in terms of space and time shortages. One limitation of this present study is that, unfortunately, it was impossible for the research team to conduct additional rounds of experiments in different times/days, locations, and under different filtration conditions. As stated in the method section, the HEPA filter bank used in the experiments was brand-new. With time and as the filter gets loaded, the performance of the HEPA air purifier is reduced due to lower air flowrates and higher pressure differentials across the loaded filter.

The temporary anteroom’s performance was very promising. Even in the absence of portable air filters the plastic barrier could prevent up to 80% of the surrogate particles from spreading to adjacent spaces. When combined with a portable HEPA air purifier, aerosol containment raised to more than 99% which is outstanding performance. In general, the portable HEPA air purifier limited aerosol dispersion via two distinct mechanisms (a) by removing the particles from the air, and (b) by creating a negative pressure across the plastic barrier. The negative pressure forces the particles to stay within the isolation space. It is important to note that these two mechanisms are independent and one must not be mistaken by the other. For example, in this work, cases with similar pressure differential were shown to have performed differently. This is because the negative pressure magnitude is largely governed by the leakiness of the space. Negative pressure was shown to be very

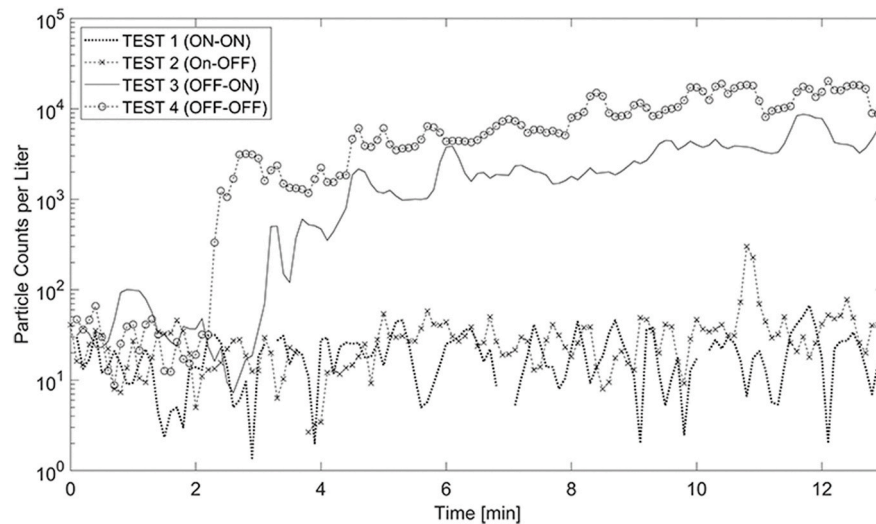


Fig. 7. Counts of Particles per liter in the Anteroom for Various HEPA Filtration Settings.

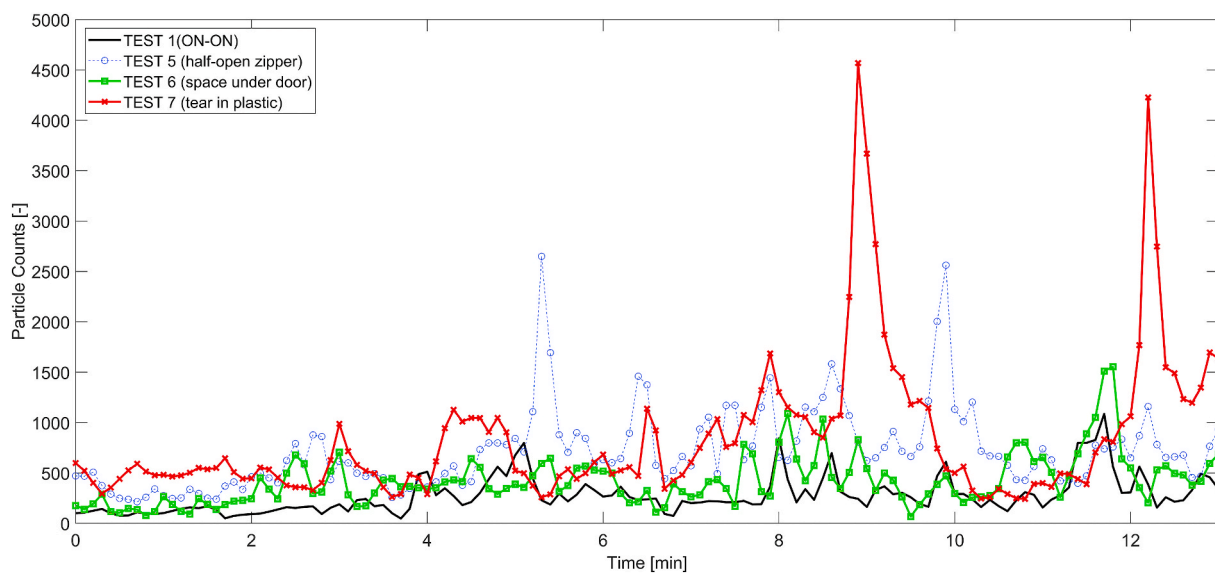


Fig. 8. Particle concentrations for cases with damage in the plastic barrier.

effective, however over pressurization did not seem to provide additional improvement.

For this study, two portable HEPA air purifiers were used. Rather obviously, the best outcome was achieved when both machines were operating. However, one would wonder where the optimum location is for the HEPA machine had there been only one available. This work shows clearly, that the best location for a single HEPA machine is inside the isolation space. In fact, placing the HEPA in the anteroom alone resulted in adverse outcomes as it drew aerosols outside of the isolation space. Another practical question is would it be best if two HEPA machines were both placed inside the isolation space? While this work did not specifically test this scenario, the answer would be no. Practically, too much negative pressure can easily collapse the plastic barrier. During the experiments, the research team aimed at increasing the ΔP to -20Pa . Shortly after, the shores began to loosen and the plastic wall started to wrinkle like a plastic bag on a vacuum. Therefore, the best performance of this temporary solution was achieved when two portable HEPA filters were placed on either side of the plastic wall. Logistically, healthcare facilities would prefer to allocate only one HEPA air purifier to each room to obtain a higher overall surge capacity, in which case, the

unit's optimal placement is inside the isolation space and possibly close the patient's bed.

Declaration of competing interest

The authors declare that they have no known competing financial interests or personal relationships that could have appeared to influence the work reported in this paper.

References

- [1] E. Dong, H. Du, L. Gardner, An interactive web-based dashboard to track COVID-19 in real time, *Lancet Infect. Dis.* 20 (2020) 533–534, [https://doi.org/10.1016/S1473-3099\(20\)30120-1](https://doi.org/10.1016/S1473-3099(20)30120-1), 2020.
- [2] M.M. Arons, K.M. Hatfield, S.C. Reddy, et al., Presymptomatic SARS-CoV-2 infections and transmission in a skilled nursing facility, *N. Engl. J. Med.* (2020).
- [3] P. Vanhems, Fast nosocomial spread of SARS-CoV2 in a French geriatric unit Lyon Study Group on Covid-19 infection*, *Infect. Control Hosp. Epidemiol.* (2020).
- [4] N. Van Doremalen, T. Bushmaker, D.H. Morris, et al., Aerosol and surface stability of SARS-CoV-2 as compared with SARS-CoV-1, *N. Engl. J. Med.* (2020).
- [5] K.J. Godri Pollitt, J. Peccia, A.I. Ko, et al., COVID-19 vulnerability: the potential impact of genetic susceptibility and airborne transmission, *Hum. Genom.* 14 (2020) 1–7.

- [6] National Center for Immunization and Respiratory Diseases, Division of Viral Diseases, Interim Infection Prevention and Control Recommendations for Patients with Suspected or Confirmed Coronavirus Disease 2019 (COVID-19) in Healthcare Settings, Cdc, 2020.
- [7] G. Grasselli, A. Pesenti, M. Cecconi, Critical care utilization for the COVID-19 outbreak in Lombardy, Italy, *JAMA*. (2020).
- [8] A. Uppal, D.M. Silvestri, M. Siegler, et al., Critical care and emergency department response at the epicenter of the COVID-19 pandemic, *Health Aff.* (2020).
- [9] J. Willan, A.J. King, K. Jeffery, N. Bienz, Challenges for NHS hospitals during covid-19 epidemic, *BMJ* (2020).
- [10] M. Leung, A.H.S. Chan, Control and management of hospital indoor air quality, *Med. Sci. Mon. Int. Med. J. Exp. Clin. Res.* 12 (2006) SR17–R23.
- [11] AIA, Guidelines for Design and Construction of Hospital, 2019.
- [12] R. Khera, S. Jain, Z. Lin, J.S. Ross, H. Krumholz, Evaluation of the Anticipated Burden of COVID-19 on Hospital-Based Healthcare Services across the United States, 2020.
- [13] United States General Accounting Office, Hospital Preparedness, 2003.
- [14] NIOSH. Engineering controls to reduce airborne, droplet and contact exposures during epidemic/pandemic response, *Centers Dis. Control Prev.* 2020 (2020). <http://www.cdc.gov/niosh/topics/healthcare/engcontrolsolutions/expedient-patient-isolation.html>.
- [15] E.S. Mousavi, D. Bausman, Renovation in hospitals: pressurization Strategies by healthcare contractors in the United States, *Heal Environ Res Des* 1–12 (2019).
- [16] T. Xia, A. Kleinheksel, E.M. Lee, Z. Qiao, K.R. Wigginton, H.L. Clack, Inactivation of airborne viruses using a packed bed non-thermal plasma reactor, *J. Phys. D Appl. Phys.* 52 (2019) 255201.
- [17] A.A. Aliabadi, S.N. Rogak, K.H. Bartlett, S.I. Green, Preventing airborne disease transmission: review of methods for ventilation design in health care facilities, *Adv Prev Med* 2011 (2011) 1–21, 2011, <http://www.pubmedcentral.nih.gov/articlerender.fcgi?artid=3226423&tool=pmcentrez&rendertype=abstract>.
- [18] E.S. Mousavi, K.R. Grosskopf, Secondary exposure risks to patients in an airborne isolation room: implications for anteroom design, *Build. Environ.* 104 (2016) 131–137.
- [19] S.S. Subhash, G. Baracco, K.P. Fennelly, M. Hodgson, L.J. Radonovich, Isolation anterooms: important components of airborne infection control, *Am. J. Infect. Contr.* 41 (2013) 452–455, <https://doi.org/10.1016/j.ajic.2012.06.004>, 2013.
- [20] P. Jensen, A. Lauren, A. Lambert, et al., Guidelines for preventing the transmission of *Mycobacterium tuberculosis* in health-care settings, *Centers Dis Control* 54 (2005) 1–141.
- [21] Ashrae Standard 170, Ventilation of Health Care Facilities, 2013.
- [22] W.G. Lindsley, J.S. Reynolds, J.V. Szalajda, J.D. Noti, D.H. Beezhold, A cough aerosol simulator for the study of disease transmission by human cough-generated aerosols, *Aerosol. Sci. Technol.* 47 (2013) 937–944, 2013, <http://www.tandfonline.com/doi/abs/10.1080/02786826.2013.803019>.
- [23] H.A. Elmaghaby, Y.W. Chiang, A.A. Aliabadi, Are aircraft acceleration-induced body forces effective on contaminant dispersion in passenger aircraft cabins? *Sci Technol Built Environ* 25 (2019) 858–872, <https://doi.org/10.1080/23744731.2019.1576457>, 2019.
- [24] G.N. Sze To, C.Y.H. Chao, Review and comparison between the Wells-Riley and dose-response approaches to risk assessment of infectious respiratory diseases, *Indoor Air* 20 (2010) 2–16.
- [25] E.S. Mousavi, K.R. Grosskopf, Airflow patterns due to door motion and pressurization in hospital isolation rooms, *Sci Technol Built Environ* 22 (2016) 379–384.
- [26] S. Lee, B. Park, T. Kurabuchi, Numerical evaluation of influence of door opening on interzonal air exchange, *Build. Environ.* 102 (2016) 230–242, <https://doi.org/10.1016/j.buildenv.2016.03.017>, 2016.
- [27] S. Rautiala, T. Reponen, A. Nevalainen, T. Husman, P. Kallioikoski, Control of exposure to airborne viable microorganisms during remediation of moldy buildings; report of three case studies, *Am. Ind. Hyg. Assoc. J.* 59 (1998) 455–460.
- [28] P. Kalliomäki, P. Saarinen, J.W. Tang, H. Koskela, Airflow patterns through single hinged and sliding doors in hospital isolation rooms – effect of ventilation, flow differential and passage, *Build. Environ.* 107 (2016) 154–168.
- [29] B. Zhou, L. Ding, F. Li, K. Xue, P.V. Nielsen, Y. Xu, Influence of opening and closing process of sliding door on interface airflow characteristic in operating room, *Build. Environ.* 144 (2018).
- [30] A. Remuzzi, G. Remuzzi, COVID-19 and Italy: what next? *Lancet* 395 (2020) 1225–1228, [https://doi.org/10.1016/S0140-6736\(20\)30627-9](https://doi.org/10.1016/S0140-6736(20)30627-9), 2020.
- [31] S. Volpato, F. Landi, R.A. Incalzi, A frail health care system for an old population: lesson form the COVID-19 outbreak in Italy, *J Gerontol A Biol Sci Med Sci* XX (2020) 1–2.
- [32] J. Xie, Z. Tong, X. Guan, B. Du, H. Qiu, A.S. Slutsky, Critical care crisis and some recommendations during the COVID-19 epidemic in China, *Intensive Care Med.* 46 (2020) 837–840, <https://doi.org/10.1007/s00134-020-05979-7>, 2020.
- [33] S.M. Moghadas, A. Shoukat, M.C. Fitzpatrick, et al., Projecting hospital utilization during the COVID-19 outbreaks in the United States, *Proc. Natl. Acad. Sci. U. S. A.* 117 (2020) 9122–9126.